Electrostatic Control of Conduction Type in Carbon Nanotube Field-Effect Transistors by Positively Charged Polyvinyl Alcohol Film

Shinya Aikawa,[*†‡] *Sungjin Kim,*[§] *Theerapol Thurakitseree,*[⊥] *Erik Einarsson,*[‖] *Taiki Inoue,*[§] *Shohei Chiashi,*[§] *Kazuhito Tsukagoshi,*[‡] *and Shigeo Maruyama,*[*§¶]

[†]Research Institute for Science and Technology, Kogakuin University, Hachioji, Tokyo 192-0015, Japan

[‡]WPI Center for Materials Nanoarchitectonics (WPI-MANA), National Institute for Materials Science (NIMS), Tsukuba, Ibaraki 305-0044, Japan

[§]Department of Mechanical Engineering, The University of Tokyo, Bunkyo, Tokyo 113-8656, Japan

[⊥]Program of Applied Physics, Faculty of Science, Maejo University, Chiang Mai 50290, Thailand

[‖]Department of Electrical Engineering, Department of Materials Design and Innovation, University at Buffalo, Buffalo, New York 14260, United States

[¶]Energy NanoEngineering Laboratory, National Institute of Advanced Industrial Science and Technology (AIST), Tsukuba 305-8564, Japan

KEYWORDS: single-walled carbon nanotubes, field-effect transistors, polyvinyl alcohol, conduction-type conversion, bulk/interfacial charges, electrostatic doping

ABSTRACT: Control of the electrical conduction type in single-walled carbon nanotube field-effect transistors (CNT-FETs) is essential for the realization of practical complementary CNT-based integrated circuits with low power consumption. Conduction-type conversion techniques that utilize the sensitivity of the electronic properties of CNTs to the surrounding environment have been developed to date. However, the mechanisms involved are still under discussion, particularly with respect to the use of a polymer coating. In the present study, the effect of a polyvinyl alcohol (PVA) coating on CNT-FETs was investigated in terms of bulk and interfacial charges. When the CNT channels are covered with pure PVA, the FET characteristics clearly change from unipolar p-type to ambipolar. The addition of ammonium ions (NH_4^+) in the PVA leads to further conversion to unipolar n-type conduction. The capacitance−voltage characteristics of a PVA/SiO_2 stacked capacitor indicate that a high density of positive charges is induced at the PVA/SiO_2 interface and within the bulk PVA. Electrons are electrostatically accumulated in the CNT channels due to the presence of the positive charges, and thus, stable n-type conduction of PVA-coated CNT-FETs is observed, even under ambient conditions. The mechanism for conversion of the conduction type is considered to be electrostatic doping and not charge transfer from the PVA molecules, due to the large amount of positive charges in the PVA and the weak interaction between CNTs and ammonia molecules. A blue-shift of the Raman G-band peak was observed for CNTs coated with NH_4^+-doped PVA, which corresponds to unipolar n-type CNT-FET behavior. These results confirm that electrostatic control of the conduction type in CNT-FETs can be achieved with a charged PVA passivation layer, and this is expected to lead to the realization of flexible and transparent pn complementary circuits composed of all-carbon materials.

1. INTRODUCTION

The sp^2 hybridization configuration of carbon–carbon bonds in single-walled carbon nanotubes (CNTs) and their one dimensionality in the nanoscale range make CNTs an attractive material in terms of both their unique mechanical (flexibility and robustness) and electrical (metallic or semiconducting) properties. To utilize these flexible semiconductor materials, an integrated circuit on a bendable plastic substrate has been realized using p-type CNT field-effect transistors (CNT-FETs).[1-4] To further enhance the device functionality, mechanical flexibility and optical transparency through the use of a thin polymer passivation layer and plastic substrate, CNT-FETs with n-type behavior have been an important target. Both p and n-type FETs are necessary for the realization of low-power consumption complementary circuits.

To date, n-type conversion of CNT-FETs has been reported through approaches such as the use of low work function metal electrodes,[5-8] high-κ materials as gate dielectrics or passivation layers,[9-13] chemical modification of CNT surfaces,[14-18] and polymer coatings. Among these, the polymer coating technique is a promising low-cost approach to fabricating transparent and flexible CNT-FETs.[19-21] When a CNT-FET is covered by an amine-rich polymer such as polyethylene imine, n-type conduction is observed,[22-25] whereas for a CNT-FET passivated with polymethyl methacrylate (PMMA),[4, 26, 27] polyethylene oxide,[28] polyacrylic acid[29] or poly(sodium 4-styrenesulfonate)[30], the conduction type does not change. This phenomenon could be as attributed to charge transfer between the CNTs and the polymer molecules;[28, 29, 31, 32] however, the mechanism for this conversion has yet to be clearly determined.

It has been reported that charge transfer occurs when electron donating molecules are adsorbed on the surfaces of CNTs.[33, 34] However, theoretical studies have revealed that the charge

transfer effect is rather weak due to non-covalent bonding with the CNT surface.[35-37] In addition, the charge transfer distance between a CNT and non-covalently attached NH_3 molecules is considerably shorter (0.29 nm)[38] than the water depletion layer thickness for a CNT (0.84 nm).[39] Polymer molecules dissolved in water cannot directly contact a CNT because the surface is superhydrophobic;[40, 41] therefore, charge carriers cannot be transferred to CNTs from water-soluble polymers. We have previously reported conduction-type conversion in both CNT-FETs and graphene FETs after polyvinyl alcohol (PVA) coating.[42, 43] Observation of an electron current in CNT-FETs and a shift of the Dirac point in graphene FETs are considered to be caused by electron doping in their channels. However, the detailed mechanism for electronic conduction due to the PVA coating has not been elucidated because water-soluble PVA molecules cannot be chemically adsorbed on these hydrophobic carbon surfaces.

Here, we investigate the mechanism for conduction-type conversion in a CNT-FET by PVA coating, and discuss how electron doping occurs in a CNT channel. It is our assumption that charge transfer would not occur due to the weak adsorption energy of physisorbed molecules due to the superhydrophobic nature of the CNT surface. Therefore, to clarify the effect of the PVA, a stacked PVA capacitor was fabricated and the charge densities within the bulk and at the interface were estimated by capacitance–voltage (C–V) measurements. Furthermore, Raman characterization of PVA-treated CNTs was performed to evaluate the carrier doping density.

2. EXPERIMENTAL SECTION

A p-type Si substrate with a 600 nm thick thermal oxide layer was first cleaned using a standard process of ultrasonication in acetone and isopropyl alcohol, followed by exposure to UV–

plasma. A patterned cobalt catalyst (nominal thickness: 0.2 nm) for CNT growth was then deposited on the substrate by RF magnetron sputtering using photolithography and a lift-off process. The CNTs were synthesized by alcohol catalytic chemical vapor deposition (ACCVD) at 800 °C for 10 min. The details of the CNT synthesis have been described in previous reports.[44, 45] The CNTs were characterized using SEM (Hitachi S-4800) and resonance Raman spectroscopy (homemade system based on Seki Technotron STR-250). Sulfur and naphthalene crystals were used to calibrate the Raman spectra for high accuracy prior to measurements. Raman spectra were measured at room temperature using an excitation wavelength of 488 nm with 1200 line/mm gratings.

A 10 wt% aqueous solution of PVA was prepared by dissolving PVA powder (Wako Pure Chemical Industries, Ltd., molecular weight: 1500) in distilled water and heating overnight at 80 °C with stirring. The solution was then degassed by ultrasonication. A PVA layer was formed by drop-casting the PVA solution onto the channel region. The substrate was then annealed at 65 °C for 10 min to solidify the PVA. The electrical characteristics of the CNT-FETs were measured using a semiconductor parameter analyzer (Agilent 4156C) at room temperature under ambient conditions. Fabrication of the air-exposed CNT-FETs with a stacked PVA/SiO_2 dielectric layer was achieved by spin-coating the PVA solution on the patterned CNT-FETs and heating for solidification of the PVA. SiO_2 and Au layers were deposited using RF magnetron sputtering under an Ar/O_2 gas mixture and vapor deposition in a thermal evaporator, respectively. The CNT-FETs were then peeled off from the Si substrate support and placed again on the substrate for the *I*-*V* measurement. The scheme is shown in Figure S1 in Supporting Information.

Au/PVA/SiO_2/p-Si stacked capacitors were fabricated using p-type Si substrates (SiO_2 thickness: 250 nm) with a resistivity of 0.5 to 0.6 Ω cm. The substrate was first cleaned using a

standard process of ultrasonication in acetone and isopropyl alcohol, followed by exposure to UV–plasma. The PVA solution was then spin-coated at various rotation speeds and dried on a hot plate at 65 °C for 10 min. A 50 nm thick Au electrode was then deposited on the PVA through a stencil shadow mask using a thermal evaporator. The PVA film thicknesses were measured using a stylus surface profiler (Dektak 6M). *C–V* measurements were performed using a precision LCR meter (Agilent E4980A) at room temperature in the dark under ambient conditions. An AC voltage of 0.5 V with a frequency of 10 kHz was superimposed on the DC bias voltage.

3. RESULTS AND DISCUSSION

Figures 1(a) and 1(b) show a schematic illustration of a PVA-coated CNT-FET and a scanning electron microscopy (SEM) image of the channel region. CNT-FETs with CNT-network source and drain electrodes were fabricated on a SiO_2/Si substrate using a photolithographically patterned CNT growth technique.[42] For the growth conditions and device dimensions used in this study (channel length L = 10 μm, electrode width W = 5 μm), the number of CNT channels was one or two.[46, 47] The electrical properties of the CNT-FETs, from unipolar p-type to ambipolar behavior without and with a PVA layer, respectively, are shown in Fig. 1(c). The influence of the PVA coating on the channel region is clearly reflected by the electrical properties of the CNT-FET. Prior to PVA coating, the FET exhibited unipolar p-type conduction, and no electron current flow occurred in the positive gate voltage (V_G) region under the measurement conditions used (drain voltage V_D = −1 V, V_G = ±10 V). In contrast, an electron current was observed after the PVA coating, similar to our previous report.[42] This ambipolar conversion is reproducible, and similar trends were observed in all FETs fabricated in this work.

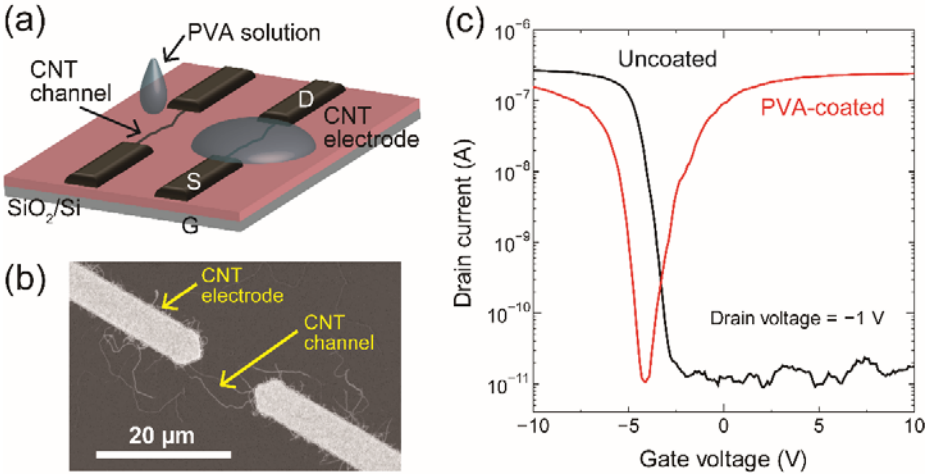

Figure 1. (a) Schematic of PVA-coated CNT-FET. The SiO_2/Si substrate is employed as a gate insulator/gate electrode (denoted as G), whereas the CNT network acts as source (S) and drain (D) electrodes, and a semiconducting channel. PVA solution is dropped on the channel region and heated for solidification. (b) SEM image of the channel region before PVA coating. (c) Typical transfer characteristics of an uncoated FET (black) and a PVA-coated FET (red). The device was measured at room temperature under ambient conditions.

The field-effect mobility in the linear regime (μ_{FE}) was estimated in both cases using the following equation:

$$\mu_{FE} = \frac{\partial I_D}{\partial V_G} \frac{L}{W C_{ox} V_D}, \quad (1)$$

where C_{ox} is the capacitance per unit area, which in this case is estimated to be 5.76×10^{-9} F/cm^2 based on a dielectric constant of 3.9 for SiO_2. For the uncoated CNT-FET, μ_{FE} is 81.2 cm^2/Vs, while for the PVA-coated CNT-FET, μ_{FE} for holes and electrons is estimated to be 26.1 and 42.4 cm^2/Vs, respectively. The subthreshold swing (ss) for the uncoated FET, hole accumulation and electron accumulation regimes for the PVA-coated FET are 0.6, 0.45 and 0.75 V/dec, respectively.

This slight improvement in the *ss* for the hole accumulation regime, despite a decrease in μ_{FE}, will be discussed later. In the case of back and forth sweep I_D-V_G measurements, hysteresis behavior was observed for both the uncoated and PVA-coated FETs (Figure S2). A reduction in the hysteresis window was observed after PVA coating, which is possibly due to the passivation effect of PVA.

To elucidate the conduction-type conversion in terms of impurity charges, capacitor structures with and without a PVA layer were fabricated, and the charge densities in the PVA bulk and at the PVA/SiO_2 interface were then estimated. Figure 2(a) shows the *C–V* characteristics of the capacitors with and without a PVA layer, which are represented as Au/PVA/SiO_2/p-Si and Au/SiO_2/p-Si, respectively. The insets show schematic cross-sectional diagrams of the stacked structures. The fabrication and characterization processes are presented in the experimental section. The thick PVA layer decreased the capacitance significantly because the capacitance was inversely proportional to the distance between the electrodes. The flatband voltage (V_{FB}) was estimated by the flatband capacitance (C_{FB}) method, of which the details can be found in the literature.[12, 48] In the case of the PVA/SiO_2 stacked capacitor, V_{FB} can be represented by:

$$V_{FB} = -\frac{1}{2\varepsilon_{ox}}\rho_{PVA}t_{PVA}^2 - \frac{1}{\varepsilon_{ox}}\left(Q_{PVA} + Q_{SiO_2}\right)t_{PVA} + \phi_{ms} - \frac{1}{\varepsilon_{ox}}Q_{SiO_2}t_{SiO_2}, \qquad (2)$$

where ϕ_{ms} is the work-function difference between the metal (Au) and the semiconductor (p-Si), ε_{ox} is the permittivity of SiO_2, ρ_{PVA} is the bulk charge density in the PVA, Q_{PVA} and Q_{SiO2} are the charge densities at the PVA/SiO_2 and SiO_2/p-Si interfaces, respectively, and t_{PVA} and t_{SiO2} are the thicknesses of the PVA and SiO_2 insulators, respectively. The details of Eq. (2) for a stacked capacitor are described in the Supporting Information (Figure S3). The two capacitors of SiO_2 and PVA are connected in series; therefore, C_{FB} with the PVA layer ($C_{FB,PVA}$) is given by:

$$C_{\mathrm{FB,PVA}} = \left\{\frac{1}{C_{\mathrm{FB}}} + \frac{1}{C_{\mathrm{PVA}}}\right\}^{-1}, \quad (3)$$

where C_{PVA} is the capacitance of the PVA, which is determined by $C_{\mathrm{PVA}} = \varepsilon_0\varepsilon_{\mathrm{PVA}}/t_{\mathrm{PVA}}$. Here, the dielectric constant for the PVA ($\varepsilon_{\mathrm{PVA}}$) is estimated to be 5.6 using a Au/PVA (1.81 μm)/SiO_2 (235 nm)/p^{++}-Si structure, where the capacitance of the PVA was measured to be 27.6 pF/mm^2 (Figure S4). Note that unlike in other *C*–*V* measurements, a heavily doped Si substrate was used to estimate $\varepsilon_{\mathrm{PVA}}$. Figure 2(b) shows the relationship between V_{FB} and the PVA thickness with the best fitted quadratic curve. Using Q_{SiO2} (-8.7×10^{11} cm^{-2}) calculated from the relationship between V_{FB} and Q_{SiO2} in the case of the Au/SiO_2/p-Si capacitor (calculation details shown in Figure S5 and Table S1 of Supporting Information), ρ_{PVA} and Q_{PVA} were estimated to be 3.6×10^{15} cm^{-3} and 5.4×10^{11} cm^{-2}, respectively. This ρ_{PVA} value corresponds to an areal density of 10^{11} cm^{-2} (the PVA thickness in this study is ca. 1 μm), which is considerably high for a bulk charge density. The bulk charge density in thermally-grown SiO_2 is typically negligible when compared with the interface charge density.[49, 50] However, the PVA has a high density of positive bulk charge; therefore, we focused on the bulk charge in addition to the interface charge density in this work.

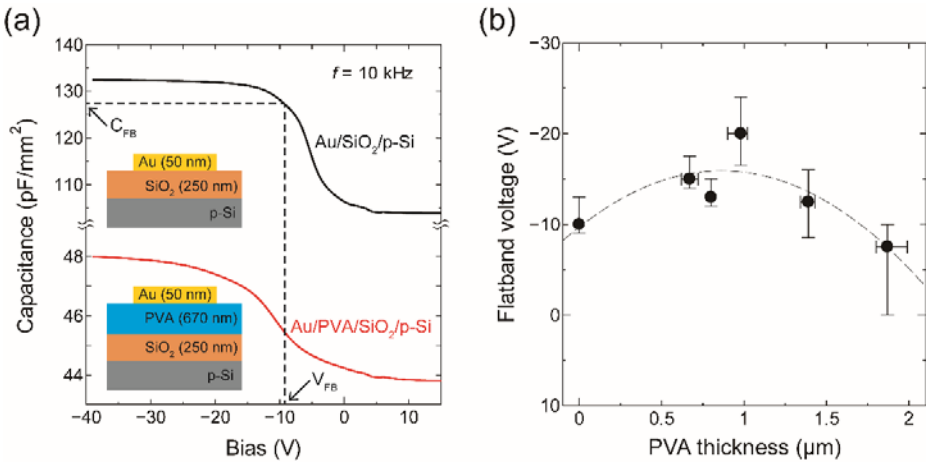

Figure 2. (a) Typical *C*–*V* characteristics for capacitors with and without a PVA layer. V_{FB} was estimated by the C_{FB} method. The insets show schematic cross-sectional diagrams of the

stacked capacitor structures. The PVA thickness estimated using a stylus surface profiler was 670 nm. The frequency for the *C*–*V* measurements was fixed at 10 kHz. (b) Estimated V_{FB} as a function of the PVA thickness. The dashed line represents the quadratic fitting curve. Based on the best fitting line, the bulk charges within PVA and at the PVA/SiO_2 interface are positively induced. The error bars are the maximum and minimum values of the 5 measured samples for each PVA spin-coating condition, while the data points represent the average value.

The ambipolar conversion of the PVA-coated CNT-FET was considered in terms of the high density of positive charges within the PVA bulk and at the PVA/SiO_2 interface. Figures 3(a) and 3(b) show schematic cross-sectional diagrams of the CNT-FET when V_G is applied. In case of $V_G < V_{th}$ (threshold voltage), holes are accumulated in the semiconducting CNT channel, similar to the case for an uncoated CNT-FET [Fig. 3(c)]; however, the accumulated carrier density is slightly suppressed in comparison with that for uncoated FETs due to the presence of electrons in the CNT channel induced by the positive bulk and interfacial charges. In addition, the CNT channel is not placed on the PVA but surrounded by the PVA, and the surrounding structure enhances carrier accumulation. The positive charges in the PVA quickly deplete the accumulated holes, so that *ss* is strongly dependent on V_G. With the improvement in *ss* due to the PVA coating effects, V_{th} is negatively shifted and the on-state current is slightly decreased, as shown in Fig. 1(c). This behavior can be explained by the electrostatic doping of electrons in the CNT channel due to the surrounding PVA with positive charges. In contrast, when $V_G > V_{th}$ [Fig. 3(d)], electrons are accumulated in the CNT channel because of the bulk and interfacial charges; therefore, an electron current was observed. In addition to its role as a positively charged layer, PVA is employed as a

passivation film that can prevent electron trapping by ambient water molecules, which results in a reduction in the hysteresis window (Figure S2).[20] Although the surrounding PVA layer includes water molecules in its composition, the amount of electron trapping molecules that interact with a CNT is considered to be low compared with that for an uncoated FET structure.

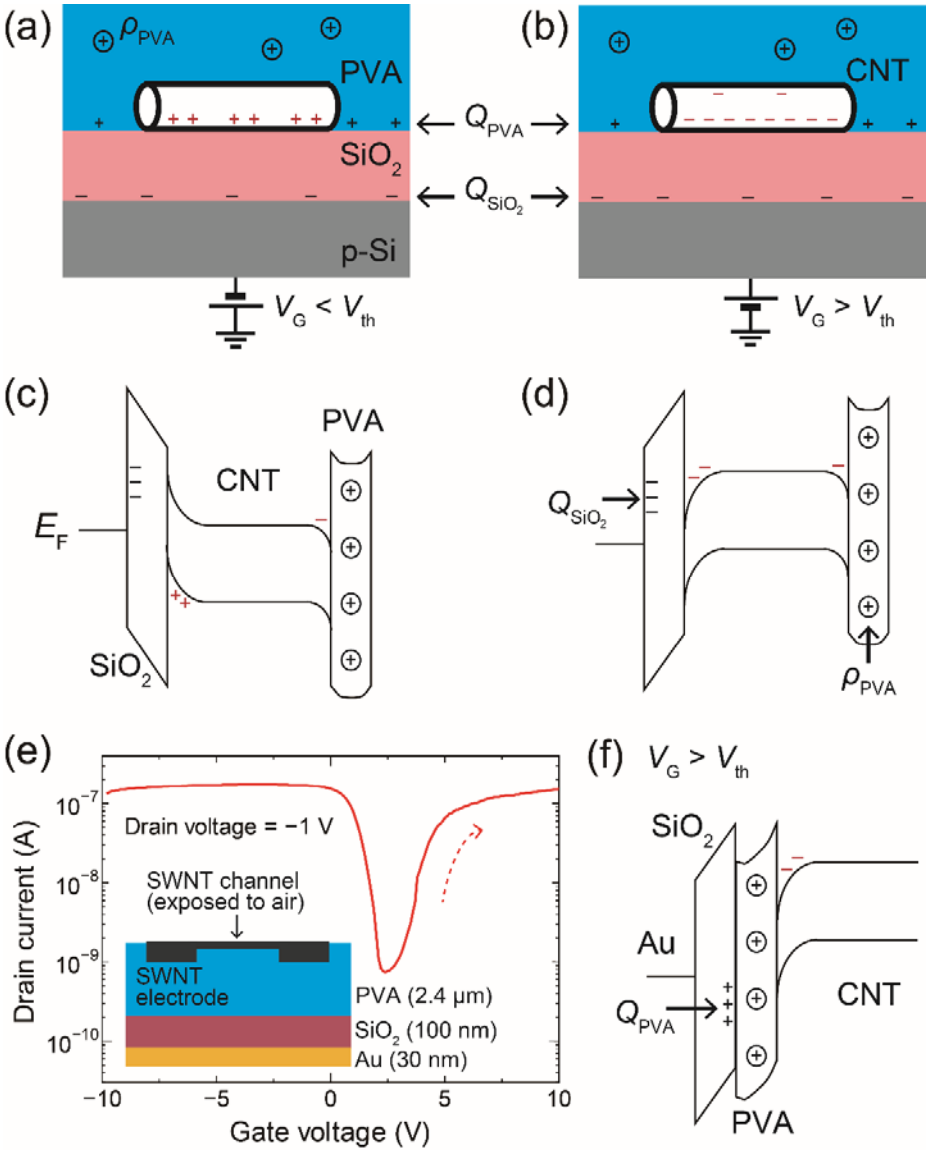

Figure 3. (a,b) Schematic cross-sectional diagrams of a PVA-coated CNT-FET with applied $V_G < V_{th}$ and $V_G > V_{th}$. ρ_{PVA}, Q_{PVA}, and Q_{SiO2} are the bulk charge density in the PVA layer,

and the charge densities at the PVA/SiO_2 and SiO_2/p-Si interfaces, respectively. The bulk charge-induced and bias-induced charges are accumulated in the CNT. (c,d) Possible band diagrams for the bias voltage application shown in (a) and (b). (e) Transfer characteristics for the CNT-FET with a stacked PVA/SiO_2 dielectric layer fabricated by the peel-off technique. The channel region is exposed to the air, as shown in the inset. The gate voltage sweep is from −10 to +10 V, similar to that for the other measurement conditions. (f) Electron accumulation band bending structure when $V_G > V_{th}$ in the air-exposed CNT-FET with the stacked dielectric layer.

According to related work that discussed a similar unipolar–ambipolar conversion using a hydrophilic/hydrophobic substrate surface, the contribution of surrounding water molecules on the hydrophilic substrate is quite large.[20] Water molecules can withdraw electrons; therefore, only p-type behavior has been obtained on a hydrophilic substrate.[51] However, the surface of PVA is superhydrophilic due to OH termination. To confirm the carrier accumulation in the CNT channel caused by the positive charges in the PVA, we measured the electrical properties of a CNT-FET with a stacked PVA/SiO_2 dielectric layer where the CNT channel was exposed to the ambient air. Figure 3(e) shows the transfer characteristics obtained and a schematic cross-sectional diagram of the FET in the inset. Ambipolar behavior was observed, although the top PVA dielectric surface was hydrophilic. This can be reasonably understood by the presence of positive charges in the dielectric PVA layer because the positively charged PVA induces electron accumulation in the CNT channel with $V_G > V_{th}$, as shown in Fig. 3(f). Observation of an electron current in the CNT-FETs fabricated on the hydrophilic PVA surface suggests that the density of positive charges in the PVA is much higher than that of electron trapping molecules. Although the sweep direction

of V_G (−10 to +10 V) was the same as that for the FET measurement condition shown in Fig. 1, V_{th} was positively shifted with the stacked PVA/SiO_2 dielectric layer. The counter-clockwise hysteresis (Figure S6) is possibly caused by a ferroelectric polarization effect of the PVA.[52, 53] The dipole behavior is pronounced when the PVA is used as a gate dielectric.

The positive bulk and interfacial charges induce electron accumulation, so that the unipolar p-type CNT-FETs were converted to ambipolar. If the positive charge density is further increased by the introduction of additional molecules, then the hole current is possibly reduced, and unipolar n-type conduction would be realized. Here, ammonium ion (NH_4^+) was selected as an additive and it was added into the PVA (denoted as PVA:NH_4^+) for conversion to unipolar n-type conduction. The PVA:NH_4^+ polymer solution was prepared by adding 0.5 mmol of ammonia solution (25% v/v, Wako Pure Chemical Industries, Ltd.) to the 10 wt% PVA solution and mixed by ultrasonication. Figure 4(a) shows the transfer characteristics of the CNT-FET before and after the PVA:NH_4^+ coating. The hole current in the FET is completely suppressed and the electrical behavior is clearly converted to unipolar n-type from p-type. The n-type operation was stable under ambient conditions, which could be attributed to the dense PVA matrix where NH_4^+ is well embedded in the polymer chain and the dense matrix prevents reaction with the ambient air.[54, 55] NH_4^+ can act as a proton donor in PVA;[56] therefore, the PVA:NH_4^+ layer itself is expected to exhibit p-type behavior if a sufficient amount of NH_4^+ is added, although its conductance would be much lower than that for a semiconducting CNT. This assumption is clearly reflected in the *C*–*V* characteristics in Fig. 4(b). The curve is very different to that for the undoped PVA [Fig. 2(a)] because the metal/insulator/semiconductor capacitor changes to a semiconductor/insulator/semiconductor (SIS) capacitor with an increase in the positive charge density in PVA. The *C*–*V* measurements indicate that the PVA is more positively charged by NH_4^+

doping than pure PVA, which results in the suppression of hole accumulation in the CNT channel caused by the Fermi level (E_F) shift toward the conduction band edge. Peng et al. suggested that the E_F shift can be attributed to charge transfer between the CNTs and adsorbed NH_3.[34] However, NH_3−CNT interaction is very weak, so that no significant charge transfer occurs between them.[35, 37] Even if NH_3 gas is diffused out from PVA and the gas molecules adsorb on defect sites of CNTs, NH_3 cannot bind to the surface, even at room temperature and despite the existence of dangling bonds, due to the low adsorption energy of NH_3.[57] Furthermore, in the case of NH_3 dissolved in water, the device sensitivity to NH_3 is pronounced because NH_3 in the gaseous and aqueous phases causes different device responses.[33, 34] This situation is similar to the PVA-coated CNT-FET structure where the PVA layer includes water molecules. In this case, NH_3 is ionized to NH_4^+ and the surrounding water layer is positively charged; therefore, the E_F shift is electrostatically induced by the surrounding charges. This is consistent with electron injection at the contact interface due to the change in the Schottky barrier height (SBH), as reported previously.[58-60] Positive charges in the PVA induce electron accumulation and an E_F shift; therefore, the SBH is modulated. Even with the CNT-CNT contact configuration used in this study, this modulation can be considered to be similar to that for a conventional metal-CNT contact.[36] We consider that the n-type behavior can also be explained by electrostatic doping rather than by charge transfer.

In the stacked capacitor shown in Fig. 4(b), both semiconductor layers in the SIS capacitor are p-type; therefore, the SIS is denoted as a p-i-p capacitor (Figure S7 in Supporting Information for a schematic of the p-i-p capacitor behavior). When a CNT-FET was coated with a negatively charged polymer such as PMMA,[61, 62] the FET behavior maintained the initial p-type conduction and μ_{FE} was increased from 72.1 to 75.6 cm^2/Vs (Figure S8 in Supporting Information shows transfer characteristics for a PMMA-coated CNT-FET). These results suggest that the density of

the bulk/interfacial charges and the polarity of the polymer are very important for controlling the conduction type and electrical properties of polymer-coated CNT-FETs. The obtained conduction type was opposite to the polarity of the charged polymer, which indicates that the conversion mechanism is electrostatic doping. If charge transfer occurs between CNT and PVA molecules, then PVA with positive charges must enhance the initial p-type conduction.

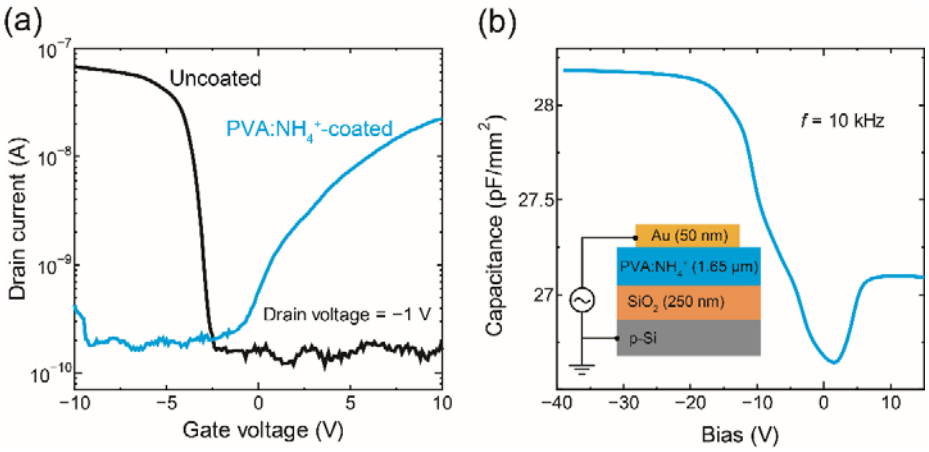

Figure 4. (a) Transfer characteristics measured at room temperature under ambient conditions for a CNT-FET before and after PVA:NH_4^+ coating. (b) *C–V* characteristics for the Au/PVA:NH_4^+/SiO_2/p-Si capacitor. The increase in the capacitance at positive bias is attributed to the heavily positive charged PVA:NH_4^+ layer, assuming that the behavior is similar to a p-i-p capacitor.

Finally, Raman spectra of the CNTs were measured in order to investigate the influence of the PVA coating. PVA-embedded CNT films were prepared for Raman spectroscopy measurements using a peel-off method (Figure S1 in Supporting Information shows a schematic of the film preparation process). The surface of the CNT film embedded in the PVA was partially

exposed to the ambient air to obtain a sufficiently strong Raman signal. When the CNT film faced the bottom Si substrate surface (the upper side has a thick PVA layer), no recognizable peaks originating from the CNTs were observed. Figure 5 shows Raman spectra for the as-grown CNTs on the SiO_2/Si substrate, and for CNT films embedded in PVA and PVA:NH_4^+. These spectra indicate that the G-peak position, originally at 1594 cm^{-1}, is blue-shifted by ca. 3 cm^{-1} with an increase in the density of electron accumulation, while there was no change in the peak width. The wavelength resolution with this Raman equipment at around 1590 cm^{-1} is 1.5 cm^{-1}; therefore, the blue-shift in the G-peak is reasonable. The shift of the G-peak with increasing accumulated carrier density occurs with both holes and electrons, and is due to a change in electron-phonon interactions.[63, 64] The Raman results for the PVA:NH_4^+-embedded CNTs are consistent with the FET properties. More positive charge doping in PVA is expected to induce more electron accumulation in a CNT channel, and consequently, the E_F shift causes a blue-shift of the G phonons. According to the calculation by Tsang et al. for a semiconducting CNT with a diameter of 2.5 nm, a Raman shift of 3 cm^{-1} at room temperature corresponds to a doping level of ca. 0.2% (1 electron per 500 carbon atoms).[61] The average diameter of the CNTs used in this work was expectedly smaller than 2.0 nm. A smaller diameter widens the bandgap; therefore, a doping concentration of more than 0.2% was possibly achieved in this case. This doping concentration can move E_F by ca. 0.3 eV toward the conduction band edge.[65] This modulation of E_F is considered to be too small for electrostatic conversion from unipolar p-type to n-type conduction.[12] However, the sample structure used for the Raman characterization is not exactly the same as that for the FET measurement; therefore, the impact on the interfacial charges (i.e., Q_{PVA} in the FET structure shown in Fig. 3) may be reduced. This is the reason why the G-peak position for the PVA-embedded CNTs appears to be the same as that for the as-grown film, although electron conduction

was observed in the PVA-coated FETs. To discuss the correlation between the FET behavior and the G-peak shift in more detail, the effect of impurity charges originating from the device structure must also be considered.

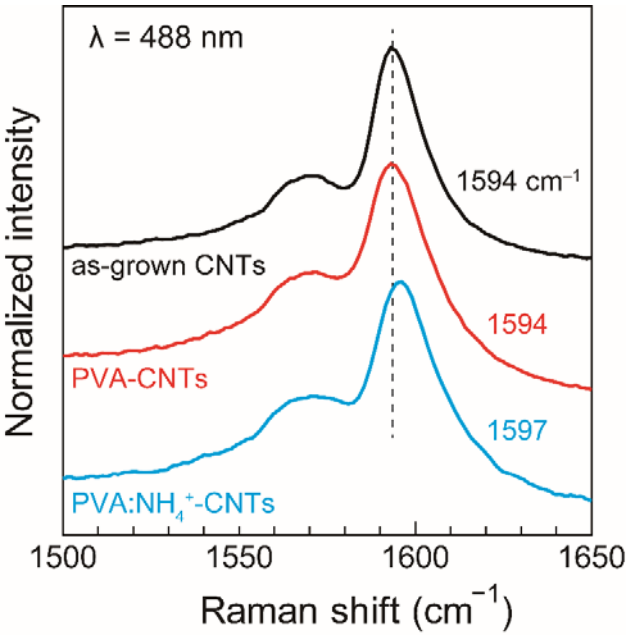

Figure 5. Resonance Raman spectra for CNT films. The black, red, and blue lines correspond to as-grown CNT film, PVA-embedded CNT film on a SiO_2/Si substrate, and a PVA:NH_4^+-embedded CNT film, respectively. The embedded samples were prepared by a peel-off method. Intensities were normalized with respect to the G-peak for comparison of the peak width. The excitation wavelength was 488 nm and the measurement was conducted at room temperature.

4. CONCLUSIONS

We have demonstrated that the conduction type in CNT-FETs can be converted using a positively charged PVA coating. When the CNT channel was covered by pure PVA, the conduction type changed from unipolar p-type to ambipolar. Conversion of the conduction type is attributed to the positive charges in PVA. Based on *C–V* measurements, the PVA has high positive charge densities in the bulk (ca. 10^{15} cm^{-3}) and at the PVA/SiO_2 interface (ca. 10^{11} cm^{-2}), which suggests that electrons are accumulated in the CNT channel electrostatically. To suppress the hole current in the PVA-coated CNT-FETs, NH_4^+ was added into the PVA solution to increase the positive charge density. A unipolar n-type CNT-FET was then demonstrated at room temperature under ambient conditions. This ability to control the conduction type can be explained in terms of electrostatic doping. If charge transfer occurs between a CNT channel and the coated PVA molecules, then PVA with positive charges must enhance the initial p-type behavior of the CNT-FET. The PVA-NH_4^+-treated CNT film caused a shift of E_F, and consequently a blue-shift of the Raman G-band peak was observed as consistent with the FET behavior. We consider that the present approach would be useful for electrostatic control and conversion of the conduction type of CNT-FETs using a PVA-based passivation layer, which could lead to the realization of flexible and transparent pn complementary circuits composed of all-carbon materials.

ASSOCIATED CONTENT

Supporting Information

Schematic diagram of sample preparation for a PVA-embedded CNT film and CNT-FETs, hysteresis window for the uncoated and PVA-coated CNT-FETs with back and forth V_G sweep, derivation of the flatband voltage as a function of the PVA thickness for a stacked capacitor,

estimation of the dielectric constant for PVA, estimation of the charge density at the SiO_2/p-Si interface (Q_{SiO2}), counter-clockwise hysteresis behavior for a CNT-FET with a stacked PVA/SiO_2 dielectric layer, schematic illustration of the p-i-p capacitor behavior, transfer characteristics of the PMMA-coated CNT-FET. This material is available free of charge via the internet at http://pubs.acs.org.

AUTHOR INFORMATION

Corresponding Authors

*E-mail: aikawa@cc.kogakuin.ac.jp

*E-mail: maruyama@photon.t.u-tokyo.ac.jp

Notes

The authors declare no competing financial interest.

ACKNOWLEDGMENTS

This work was supported by MEXT KAKENHI Grant Number 19054003 and by JSPS KAKENHI Grant Numbers 24860018, 22226006, 23760179, 23760180. This work was also supported by the VLSI Design and Education Center (VDEC), The University of Tokyo, in collaboration with Cadence Corporation.

REFERENCES

1. Cao, Q.; Kim, H. S.; Pimparkar, N.; Kulkarni, J. P.; Wang, C.; Shim, M.; Roy, K.; Alam, M. A.; Rogers, J. A., Medium-scale carbon nanotube thin-film integrated circuits on flexible plastic substrates. *Nature* **2008,** *454* (7203), 495-500.

2. Sun, D. M.; Timmermans, M. Y.; Tian, Y.; Nasibulin, A. G.; Kauppinen, E. I.; Kishimoto, S.; Mizutani, T.; Ohno, Y., Flexible high-performance carbon nanotube integrated circuits. *Nat. Nanotechnol.* **2011,** *6* (3), 156-161.

3. Wang, C.; Chien, J. C.; Takei, K.; Takahashi, T.; Nah, J.; Niknejad, A. M.; Javey, A., Extremely bendable, high-performance integrated circuits using semiconducting carbon nanotube networks for digital, analog, and radio-frequency applications. *Nano Lett.* **2012,** *12* (3), 1527-1533.

4. Sun, D. M.; Timmermans, M. Y.; Kaskela, A.; Nasibulin, A. G.; Kishimoto, S.; Mizutani, T.; Kauppinen, E. I.; Ohno, Y., Mouldable all-carbon integrated circuits. *Nat. Commun.* **2013,** *4*, 2302.

5. Nosho, Y.; Ohno, Y.; Kishimoto, S.; Mizutani, T., n-type carbon nanotube field-effect transistors fabricated by using Ca contact electrodes. *Appl. Phys. Lett.* **2005,** *86* (7), 073105.

6. Nosho, Y.; Ohno, Y.; Kishimoto, S.; Mizutani, T., Relation between conduction property and work function of contact metal in carbon nanotube field-effect transistors. *Nanotechnology* **2006,** *17* (14), 3412-3415.

7. Zhang, Z.; Liang, X.; Wang, S.; Yao, K.; Hu, Y.; Zhu, Y.; Chen, Q.; Zhou, W.; Li, Y.; Yao, Y., Doping-free fabrication of carbon nanotube based ballistic CMOS devices and circuits. *Nano Lett.* **2007,** *7* (12), 3603-3607.

8. Zhang, Z.; Wang, S.; Wang, Z.; Ding, L.; Pei, T.; Hu, Z.; Liang, X.; Chen, Q.; Li, Y.; Peng, L. M., Almost perfectly symmetric SWCNT-based CMOS devices and scaling. *ACS Nano* **2009,** *3* (11), 3781-3787.

9. Javey, A.; Kim, H.; Brink, M.; Wang, Q.; Ural, A.; Guo, J.; McIntyre, P.; McEuen, P.; Lundstrom, M.; Dai, H., High-κ dielectrics for advanced carbon-nanotube transistors and logic gates. *Nat. Mater.* **2002,** *1* (4), 241-246.

10. Kaminishi, D.; Ozaki, H.; Ohno, Y.; Maehashi, K.; Inoue, K.; Matsumoto, K.; Seri, Y.; Masuda, A.; Matsumura, H., Air-stable n-type carbon nanotube field-effect transistors with Si_3N_4 passivation films fabricated by catalytic chemical vapor deposition. *Appl. Phys. Lett.* **2005,** *86* (11), 113115.

11. Zhang, Z.; Wang, S.; Ding, L.; Liang, X.; Pei, T.; Shen, J.; Xu, H.; Chen, Q.; Cui, R.; Li, Y.; Peng, L. M., Self-aligned ballistic n-type single-walled carbon nanotube field-effect transistors with adjustable threshold voltage. *Nano Lett* **2008,** *8* (11), 3696-3701.

12. Moriyama, N.; Ohno, Y.; Kitamura, T.; Kishimoto, S.; Mizutani, T., Change in carrier type in high-κ gate carbon nanotube field-effect transistors by interface fixed charges. *Nanotechnology* **2010,** *21* (16), 165201.

13. Moriyama, N.; Ohno, Y.; Suzuki, K.; Kishimoto, S.; Mizutani, T., High-Performance Top-Gate Carbon Nanotube Field-Effect Transistors and Complementary Metal–Oxide–Semiconductor Inverters Realized by Controlling Interface Charges. *Appl. Phys. Express* **2010,** *3* (10), 105102.

14. Zhou, C.; Kong, J.; Yenilmez, E.; Dai, H., Modulated Chemical Doping of Individual Carbon Nanotubes. *Science* **2000,** *290* (5496), 1552-1555.

15. Javey, A.; Tu, R.; Farmer, D. B.; Guo, J.; Gordon, R. G.; Dai, H., High performance n-type carbon nanotube field-effect transistors with chemically doped contacts. *Nano Lett* **2005,** *5* (2), 345-348.

16. Tasis, D.; Tagmatarchis, N.; Bianco, A.; Prato, M., Chemistry of carbon nanotubes. *Chem. Rev.* **2006,** *106* (3), 1105-1136.

17. Kang, B. R.; Yu, W. J.; Kim, K. K.; Park, H. K.; Kim, S. M.; Park, Y.; Kim, G.; Shin, H.-J.; Kim, U. J.; Lee, E.-H.; Choi, J.-Y.; Lee, Y. H., Restorable Type Conversion of Carbon Nanotube

Transistor Using Pyrolytically Controlled Antioxidizing Photosynthesis Coenzyme. *Adv. Funct. Mater.* **2009,** *19* (16), 2553-2559.

18. Kim, S. M.; Jang, J. H.; Kim, K. K.; Park, H. K.; Bae, J. J.; Yu, W. J.; Lee, I. H.; Kim, G.; Loc, D. D.; Kim, U. J.; Lee, E. H.; Shin, H. J.; Choi, J. Y.; Lee, Y. H., Reduction-controlled viologen in bisolvent as an environmentally stable n-type dopant for carbon nanotubes. *J Am Chem Soc* **2009,** *131* (1), 327-331.

19. Collins, P. G.; Bradley, K.; Ishigami, M.; Zettl, A., Extreme oxygen sensitivity of electronic properties of carbon nanotubes. *Science* **2000,** *287* (5459), 1801-1804.

20. Kim, W.; Javey, A.; Vermesh, O.; Wang, O.; Li, Y. M.; Dai, H. J., Hysteresis caused by water molecules in carbon nanotube field-effect transistors. *Nano Lett.* **2003,** *3* (2), 193-198.

21. Voggu, R.; Rout, C. S.; Franklin, A. D.; Fisher, T. S.; Rao, C. N. R., Extraordinary sensitivity of the electronic structure and properties of single-walled carbon nanotubes to molecular charge-transfer. *J. Phys. Chem. C* **2008,** *112* (34), 13053-13056.

22. Shim, M.; Javey, A.; Kam, N. W.; Dai, H., Polymer functionalization for air-stable n-type carbon nanotube field-effect transistors. *J. Am. Chem. Soc.* **2001,** *123* (46), 11512-11513.

23. Zhou, Y.; Gaur, A.; Hur, S.-H.; Kocabas, C.; Meitl, M. A.; Shim, M.; Rogers, J. A., p-Channel, n-Channel Thin Film Transistors and p−n Diodes Based on Single Wall Carbon Nanotube Networks. *Nano Lett.* **2004,** *4* (10), 2031-2035.

24. Kang, S. J.; Kocabas, C.; Ozel, T.; Shim, M.; Pimparkar, N.; Alam, M. A.; Rotkin, S. V.; Rogers, J. A., High-performance electronics using dense, perfectly aligned arrays of single-walled carbon nanotubes. *Nat. Nanotechnol.* **2007,** *2* (4), 230-236.

25. Hur, S. H.; Kocabas, C.; Gaur, A.; Park, O. O.; Shim, M.; Rogers, J. A., Printed thin-film transistors and complementary logic gates that use polymer-coated single-walled carbon nanotube networks. *J. Appl. Phys.* **2005,** *98* (11), 114302.

26. Derycke, V.; Martel, R.; Appenzeller, J.; Avouris, P., Carbon nanotube inter- and intramolecular logic gates. *Nano Lett.* **2001,** *1* (9), 453-456.

27. Thanh, Q. N.; Jeong, H.; Kim, J.; Kevek, J. W.; Ahn, Y. H.; Lee, S.; Minot, E. D.; Park, J. Y., Transfer-Printing of As-Fabricated Carbon Nanotube Devices onto Various Substrates. *Adv. Mater.* **2012,** *24* (33), 4499-4504.

28. Ozel, T.; Gaur, A.; Rogers, J. A.; Shim, M., Polymer electrolyte gating of carbon nanotube network transistors. *Nano Lett.* **2005,** *5* (5), 905-911.

29. Siddons, G. P.; Merchin, D.; Back, J. H.; Jeong, J. K.; Shim, M., Highly efficient Gating and doping of carbon nanotubes with polymer electrolytes. *Nano Lett.* **2004,** *4* (5), 927-931.

30. Bradley, K.; Cumings, J.; Star, A.; Gabriel, J. C. P.; Gruner, G., Influence of mobile ions on nanotube based FET devices. *Nano Lett.* **2003,** *3* (5), 639-641.

31. Zhu, J.; Shim, B. S.; Di Prima, M.; Kotov, N. A., Transparent conductors from carbon nanotubes LBL-assembled with polymer dopant with π-π electron transfer. *J. Am. Chem. Soc.* **2011,** *133* (19), 7450-7460.

32. Klinke, C.; Chen, J.; Afzali, A.; Avouris, P., Charge transfer induced polarity switching in carbon nanotube transistors. *Nano Lett.* **2005,** *5* (3), 555-558.

33. Bradley, K.; Gabriel, J. C.; Briman, M.; Star, A.; Gruner, G., Charge transfer from ammonia physisorbed on nanotubes. *Phys. Rev. Lett.* **2003,** *91* (21), 218301.

34. Peng, N.; Zhang, Q.; Chow, C. L.; Tan, O. K.; Marzari, N., Sensing Mechanisms for Carbon Nanotube Based NH_3 Gas Detection. *Nano Lett.* **2009,** *9* (4), 1626-1630.

35. Bai, L.; Zhou, Z., Computational study of B- or N-doped single-walled carbon nanotubes as NH_3 and NO_2 sensors. *Carbon* **2007,** *45* (10), 2105-2110.

36. Li, Y.; Hodak, M.; Lu, W.; Bernholc, J., Mechanisms of NH_3 and NO_2 detection in carbon-nanotube-based sensors: An ab initio investigation. *Carbon* **2016,** *101*, 177-183.

37. Bauschlicher Jr, C. W.; Ricca, A., Binding of NH_3 to graphite and to a (9, 0) carbon nanotube. *Phys. Rev. B* **2004,** *70* (11), 115409.

38. Chang, H.; Lee, J. D.; Lee, S. M.; Lee, Y. H., Adsorption of NH_3 and NO_2 molecules on carbon nanotubes. *Appl. Phys. Lett.* **2001,** *79* (23), 3863-3865.

39. Homma, Y.; Chiashi, S.; Yamamoto, T.; Kono, K.; Matsumoto, D.; Shitaba, J.; Sato, S., Photoluminescence Measurements and Molecular Dynamics Simulations of Water Adsorption on the Hydrophobic Surface of a Carbon Nanotube in Water Vapor. *Phys. Rev. Lett.* **2013,** *110* (15), 157402.

40. Lau, K. K. S.; Bico, J.; Teo, K. B. K.; Chhowalla, M.; Amaratunga, G. A. J.; Milne, W. I.; McKinley, G. H.; Gleason, K. K., Superhydrophobic carbon nanotube forests. *Nano Lett.* **2003,** *3* (12), 1701-1705.

41. Murakami, Y.; Maruyama, S., Detachment of vertically aligned single-walled carbon nanotube films from substrates and their re-attachment to arbitrary surfaces. *Chem. Phys. Lett.* **2006,** *422* (4-6), 575-580.

42. Aikawa, S.; Einarsson, E.; Thurakitseree, T.; Chiashi, S.; Nishikawa, E.; Maruyama, S., Deformable transparent all-carbon-nanotube transistors. *Appl. Phys. Lett.* **2012,** *100* (6), 063502.

43. Kim, S.; Zhao, P.; Aikawa, S.; Einarsson, E.; Chiashi, S.; Maruyama, S., Highly Stable and Tunable n-Type Graphene Field-Effect Transistors with Polyvinyl Alcohol Films. *ACS Appl. Mater. Interfaces* **2015,** *7* (18), 9702-9708.

44. Maruyama, S.; Einarsson, E.; Murakami, Y.; Edamura, T., Growth process of vertically aligned single-walled carbon nanotubes. *Chem. Phys. Lett.* **2005,** *403* (4-6), 320-323.

45. Einarsson, E.; Kadowaki, M.; Ogura, K.; Okawa, J.; Xiang, R.; Zhang, Z.; Yamamoto, T.; Ikuhara, Y.; Maruyama, S., Growth mechanism and internal structure of vertically aligned single-walled carbon nanotubes. *J. Nanosci. Nanotechnol.* **2008,** *8* (11), 6093-6098.

46. Aikawa, S.; Einarsson, E.; Inoue, T.; Xiang, R.; Chiashi, S.; Shiomi, J.; Nishikawa, E.; Maruyama, S., Simple Fabrication Technique for Field-Effect Transistor Array Using As-Grown Single-Walled Carbon Nanotubes. *Jpn. J. Appl. Phys.* **2011,** *50* (4), 04DN08.

47. Aikawa, S.; Xiang, R.; Einarsson, E.; Chiashi, S.; Shiomi, J.; Nishikawa, E.; Maruyama, S., Facile fabrication of all-SWNT field-effect transistors. *Nano Res.* **2011,** *4* (6), 580-588.

48. Nicollian, E. H.; Brews, J. R., *MOS (metal oxide semiconductor) physics and technology*. Wiley: **1982**.

49. Kerber, A.; Cartier, E.; Pantisano, L.; Degraeve, R.; Kauerauf, T.; Kim, Y.; Hou, A.; Groeseneken, G.; Maes, H. E.; Schwalke, U., Origin of the threshold voltage instability in SiO_2/HfO dual layer gate dielectrics. *IEEE Electron Device Lett.* **2003,** *24* (2), 87-89.

50. Kaushik, V. S.; O'Sullivan, B. J.; Pourtois, G.; Van Hoornick, N.; Delabie, A.; Van Elshocht, S.; Deweerd, W.; Schram, T.; Pantisano, L.; Rohr, E.; Ragnarsson, L. A.; De Gendt, S.; Heyns, M., Estimation of fixed charge densities in hafnium-silicate gate dielectrics. *IEEE Trans. Electron Devices* **2006,** *53* (10), 2627-2633.

51. Aguirre, C. M.; Levesque, P. L.; Paillet, M.; Lapointe, F.; St-Antoine, B. C.; Desjardins, P.; Martel, R., The Role of the Oxygen/Water Redox Couple in Suppressing Electron Conduction in Field-Effect Transistors. *Adv. Mater.* **2009,** *21* (30), 3087-3091.

52. Choi, Y. S.; Sung, J.; Kang, S. J.; Cho, S. H.; Hwang, I.; Hwang, S. K.; Huh, J.; Kim, H.-C.; Bauer, S.; Park, C., Control of Current Hysteresis of Networked Single-Walled Carbon Nanotube Transistors by a Ferroelectric Polymer Gate Insulator. *Adv. Funct. Mater.* **2013,** *23* (9), 1120-1128.

53. Sun, Y.-L.; Xie, D.; Xu, J.-L.; Zhang, C.; Dai, R.-X.; Li, X.; Meng, X.-J.; Zhu, H.-W., Controllable Hysteresis and Threshold Voltage of Single-Walled Carbon Nano-tube Transistors with Ferroelectric Polymer Top-Gate Insulators. *Sci. Rep.* **2016,** *6*, 23090.

54. Korsmeyer, R. W.; Peppas, N. A., Effect of the Morphology of Hydrophilic Polymeric Matrices on the Diffusion and Release of Water-Soluble Drugs. *J. Membr. Sci.* **1981,** *9* (3), 211-227.

55. Uddin, M. J.; Sannigrahi, J.; Masud, M. G.; Bhadra, D.; Chaudhuri, B. K., High dielectric permittivity and percolative behavior of polyvinyl alcohol/potassium dihydrogen phosphate composites. *J. Appl. Polym. Sci.* **2012,** *125* (3), 2363-2370.

56. Hirankumar, G.; Selvasekarapandian, S.; Kuwata, N.; Kawamura, J.; Hattori, T., Thermal, electrical and Optical studies on the poly(vinyl alcohol) based polymer electrolytes. *J. Power Sources* **2005,** *144* (1), 262-267.

57. Feng, X.; Irle, S.; Witek, H.; Morokuma, K.; Vidic, R.; Borguet, E., Sensitivity of ammonia interaction with single-walled carbon nanotube bundles to the presence of defect sites and functionalities. *J. Am. Chem. Soc.* **2005,** *127* (30), 10533-10538.

58. Peng, N.; Li, H.; Zhang, Q., Nanoscale contacts between carbon nanotubes and metallic pads. *ACS Nano* **2009,** *3* (12), 4117-4121.

59. Gui, E. L.; Li, L.-J.; Zhang, K.; Xu, Y.; Dong, X.; Ho, X.; Lee, P. S.; Kasim, J.; Shen, Z. X.; Rogers, J. A.; Mhaisalkar, DNA Sensing by Field-Effect Transistors Based on Networks of Carbon Nanotubes. *J. Am. Chem. Soc.* **2007,** *129* (46), 14427-14432.

60. Chan, M. Y.; Wei, L.; Chen, Y.; Chan, L.; Lee, P. S., Charge-induced conductance modulation of carbon nanotube field effect transistor memory devices. *Carbon* **2009,** *47* (13), 3063-3070.

61. Yilmaz, E.; Sezen, H.; Suzer, S., Probing the charge build-up and dissipation on thin PMMA film surfaces at the molecular level by XPS. *Angew. Chem. Int. Ed.* **2012,** *51* (22), 5488-5492.

62. Albrecht, V.; Janke, A.; Nemeth, E.; Spange, S.; Schubert, G.; Simon, F., Some aspects of the polymers' electrostatic charging effects. *J. Electrostat.* **2009,** *67* (1), 7-11.

63. Tsang, J. C.; FreitagM; PerebeinosV; LiuJ; AvourisPh, Doping and phonon renormalization in carbon nanotubes. *Nat. Nanotechnol.* **2007,** *2* (11), 725-730.

64. Suzuki, S.; Hibino, H., Characterization of doped single-wall carbon nanotubes by Raman spectroscopy. *Carbon* **2011,** *49* (7), 2264-2272.

65. Das, A.; Sood, A. K.; Govindaraj, A.; Saitta, A. M.; Lazzeri, M.; Mauri, F.; Rao, C. N. R., Doping in carbon nanotubes probed by Raman and transport measurements. *Phys. Rev. Lett.* **2007,** *99* (13).

TABLE OF CONTENTS GRAPHIC